Chemical Physics Letters 509 (2011) 169–174

Contents lists available at ScienceDirect

Chemical Physics Letters

journal homepage: www.elsevier.com/locate/cplett

A quantum mechanical/molecular mechanical study of the aspartic protease plasmepsin IV complexed with allophenylnorstatine-based inhibitor

Natália de Farias Silva [a], Jerônimo Lameira [a,b], Cláudio Nahum Alves [a,*]

[a] Laborátorio de Planejamento e Desenvolvimento de Fármacos, Instituto de Ciências Exatas e Naturais, Universidade Federal do Pará (UFPA), 66075-110 Belém, PA, Brazil
[b] Faculdade de Biotecnologia, Instituto de Ciências Biológicas, Universidade Federal do Pará (UFPA), 66075-110 Belém, PA, Brazil

ARTICLE INFO

Article history:
Received 30 January 2011
In final form 27 April 2011
Available online 30 April 2011

ABSTRACT

Plasmepsin IV (PM IV) is a potential target for developing drugs against malaria. This Letter presents results of QM/MM dynamic simulations applied to the study of the protonation state of two aspartates (Asp34 and Asp214) catalytic residues of PM IV in complex with KNI-764 inhibitor. The potential of mean force profile was used to assign the protonation state of the two catalytic aspartates in PM IV–KNI-764 complex. The results indicate that protonation of the 214 residue is more favorable. In addition, energy terms decomposition was used to explore key interactions between the main residues and KNI-764 inhibitor.

1. Introduction

Malaria is the largest tropical parasitic disease in the world, with the continents most affected being Africa, some regions of Asia, Central and South America and some Caribbean Islands. Data from the World Health Organization (WHO) suggest an estimated 300–660 million cases recorded yearly around the world, with an annual occurrence of mortality in excess of 2.5 million [1,2]. The agent that causes malaria in humans belongs to the genus of protozoa known as *Plasmodium,* four types of which infect humans: *P. falciparum, P. vivax, P. malariae and P. ovale,* with the first being the greatest cause of deaths in humans [3]. The parasite causes the disease during its intra-erythrocytic cycle, by consuming human hemoglobin for its growth and maturation. The degradation of hemoglobin is performed by a number of proteases called plasmepsins in acid food vacuoles [4].

Different plasmepsin molecules have been identified in the *P. falciparum* genome and four of them are active in the food vacuole during the intra-erythrocytic stage. The Plasmepsin molecules are also capable of several other cleavages after the initial event [5,6]. These enzymes have similarities, which can demonstrate biological activities that are of interest for research [7,8].

Recently, the first PM IV crystallography of the enzyme complexed with an allophenylnorstatine inhibitor was reported by Clement and co-workers [9]. The great interest in this class of inhibitors is due to their efficiency in front of the enzymes in the *P. falciparum* [10] food vacuole, and the original purpose for this inhibitor is considered to be the inhibition of HIV-1 protease enzymes [11,12]. Crystallographic results were observed in the complex formed by the PM IV enzyme inhibitor KNI-764, which was in a different position from what is expected when compared to a previous model of this analysis. This new fact demonstrates the importance of further study in order to obtain a more accurate understanding of the interaction occurring in the formation of this complex [13].

Several computational methods, including molecular docking and classical molecular dynamics [4,10,14–16] simulations have been employed to elucidate the binding mode of PM inhibitors, and to calculate the free energy profile for the catalytic mechanism [17]. One option that has been utilized to accurately describe the enzyme–inhibitor complex, consists of using the protonation state from aspartates 34 and 214. Friedman and Caflisch [18] conducted studies of the PM II protonation state with classical MD simulations and obtained results in a favorable protonation to Asp214 when activating the enzyme. In a recent study, Gutiérrez-de-Terán and co-workers [14] performed a computational analysis for the PM IV–KNI-764 complex and a study was also conducted with classical MD aiming to bind affinities using linear interaction energy (LIE). The authors showed that the protonation of Asp214 favors a stable active site structure.

Recent studies have applied hybrid Quantum Mechanics/Molecular Mechanics (QM/MM) methodology with great success in the study of protein–ligand interactions in the HIV-1 protease system [19], OH transfer in Flavin-dependent oxidoreductases *p*-Hydroxybenzoate hydroxylase and others [20]. When procedures using this methodology are performed, hybrid QM/MM species or substrates are described by QM. This description includes quantum effects such as ligand polarization upon binding [21], with the protein and solvent environment being represented by means of the MM force field.

* Corresponding author. Fax: +55 91 32017633.
E-mail address: nahum@ufpa.br (C.N. Alves).

0009-2614
doi:10.1016/j.cplett.2011.04.085

In this report, we used hybrid methodology QM/MM molecular dynamics (MD) simulations to study the details of the PM IV–KNI-764 interactions and investigate the protonation state of the two catalytic aspartates, Asp34 and Asp214, in PM IV–KNI-764 complex. Moreover, contribution of individual residues to the total inhibitor–protein interaction energy have been computed between KNI-764 and some key residues inside the binding pocket, as well as an estimation of the inhibitor–protein electrostatic binding free energy that was used to explain the difference in the protonation state of the Asp34 and Asp214. In addition, we have computed the potential of mean force (PMF) profile to assign the main protonation state of these aspartates in PM IV–KNI-764 complex.

2. Methodology

2.1. Model

The initial structure was constructed from the A-chain of the X-ray crystal structure complexed with the allophenylnorstatine inhibitor (KNI-764), code PBD 2ANL [9]. Once it became possible to exchange standard pK_a values of the ionisable group with local protein environments [22], an accurate assignment of the protonation states of the amino acids at pH 7 was carried out by recalculating the standard pK_a values of the titratable amino acids using the 'cluster method' [22], as implemented by Field and co-workers [23]. In this methodology, each titratable residue in the protein is perturbed by the electrostatic effects of the protein environment. We have also performed calculation of pK_a values of amino acids within the empirical *propKa* program of Li and co-workers [24].

To perform a theoretical study of an enzymatic environment QM/MM was employed using the *f*Dynamo library [29]. The PM IV enzyme consists of 327 amino acid residues, whose catalytic residues are Asp34 and Asp214, and 7 molecules of water, called water of crystallization. Its active site is composed of an inhibitor called KNI-764, which was crystallized with the enzyme, forming the enzyme–inhibitor complex. During preparation of the enzyme for the MD simulation, hydrogen atoms were added to the system, so that the pH was neutral. The system was embedded in a cubic box (80 Å side) containing 19,418 atoms in order to simulate the reaction medium. The final system contains a total of 63,515 atoms, where 83 atoms are in QM region (KNI-764 inhibitor, Asp34 and Asp214).

2.2. QM/MM MD simulations

For the hybrid QM/MM MD calculations, we have two simulation models, **A** (protonating Asp214) and **B** (protonating Asp34) (Scheme 1), where the atoms of the inhibitor and Asp214 and Asp34 were selected for treatment by QM. To saturate the valence of the QM/MM frontier in the first model, we used a link atom [25], placed between the C^{α} and C^{β} atoms of Asp214 and Asp34 residues. The semiempirical AM1 Hamiltonian was employed to describe the QM part [26], while the rest of the system (protein plus water molecules) was described using the OPLS-AA [27] and TIP3P [28] force fields, respectively, as implemented in the *f*Dynamo library [29].

Due to the amount of degrees of freedom, any residue 25 Å apart from any of the atoms of the initial inhibitor was selected to be kept frozen (which represents a total of 50,865 atoms) in the remaining calculations in order to make the model computationally feasible. Cutoffs for the non-bonding interactions were applied using a switching scheme, within a range radius from 18.0 to 14.5 Å.

Once the systems were pre-equilibrated, 1.6 ns of QM/MM MD were run at a temperature of 300 K. The computed RMSD for the protein during the last 100 ps rendered a value that was always below 0.8 Å, while the RMS of the temperature along the different equilibration steps was always lower than 2.5 K and the variation coefficient of the potential energy during the dynamics simulations was never greater higher than 0.3%. The potential energy of our scheme [30] is derived from the standard QM/MM formulation (for more details see Ref. [30]). In addition, it must be pointed out that, because the use of high level Hamiltonians for performing hybrid MD is currently prohibitive, the electrostatic free energy has been evaluated using the semiempirical AM1 Hamiltonian. In addition, the interaction energy between the inhibitor and the environment was computed by residue, where the atoms of the inhibitor and Asp214 and Asp34 were selected for treatment using QM. Finally, the internal energy and the contribution of individual amino acid residues were calculated using the hybrid density functional theory (DFT) [31], where the B3LYP functional within the 6-31G(d,p) basis set has been employed to perform QM/MM

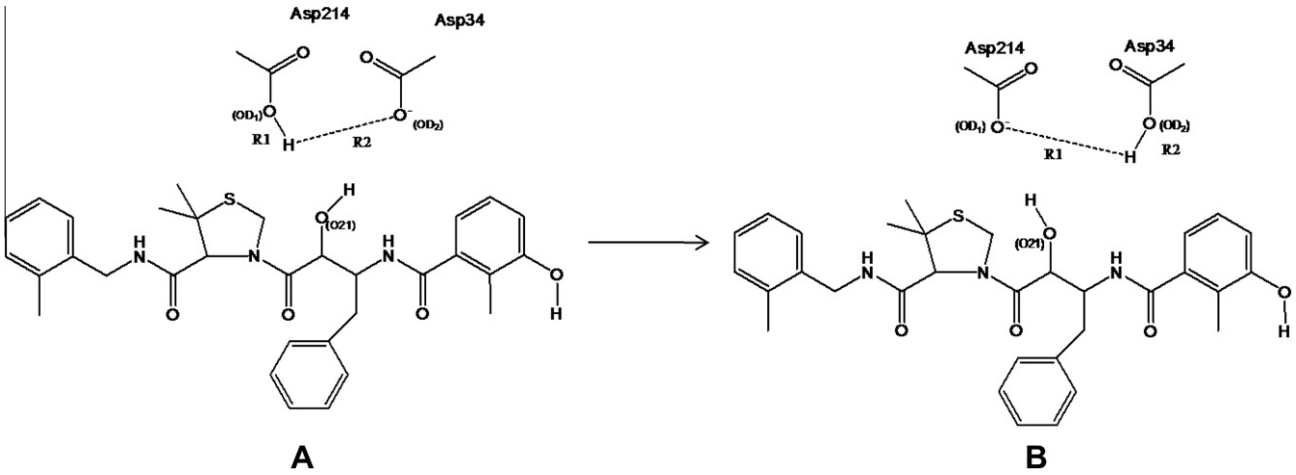

Scheme 1. Structures of the **A** and **B** models, where HE1-OD1 of Asp214 (R1) and HE2-OD2 of Asp34 (R2) coordinates corresponding to the proton transfer from Asp214 to Asp34 in 2D.

internal energy calculations in order to evaluate the appropriateness of the AM1/MM potentials for describing the non-bonded interactions between the inhibitor and the protein.

2.3. Potential of Mean Force

In order to obtain the free energy change associated to the proton transfer from Asp214 to Asp34 (transformation between **A** and **B** forms), we have computed the corresponding potential of mean force (PMF) [32] using the weighted histogram analysis method (WHAM) combined with the umbrella sampling approach [33] as implemented in *f*Dynamo [29]. In this PMF, the distinguishing reaction coordinates was the antisymmetric combination of the distances HE1-OD1 of Asp214 (R1) and HE2-OD2 of Asp34 (R2) coordinates (see Scheme 1) corresponding to the proton transfer from Asp214 to Asp34. A total of 40 simulations were performed at different values of R1 and R2 (in a range from −1.5 to +1.5 Å), with an umbrella force constant of 2800 kJ mol^{-1} A^{-2}. In each window, 5 ps of relaxation were followed by 10 ps of production QM/MM MD with a time step of 0.5 ps due to the nature of the chemical step involving a hydrogen transfer.

Table 1
Binding free energies ($\Delta G_{Elect\ -\ AM1/MM}$) obtained from electrostatic FEP calculations at the AM1/MM level and averaged interaction energies computed during the last 100 ps of AM1/MM MD simulations ($E_{Elect\ -\ AM1/MM}$).

Energies (in kJ mol^{-1})	Model	
	A	**B**
$\Delta G_{Elect\ -\ AM1/MM}$	−136.42	−125.30
$E_{Elect\ -\ AM1/MM}$	−581.21	−530.80

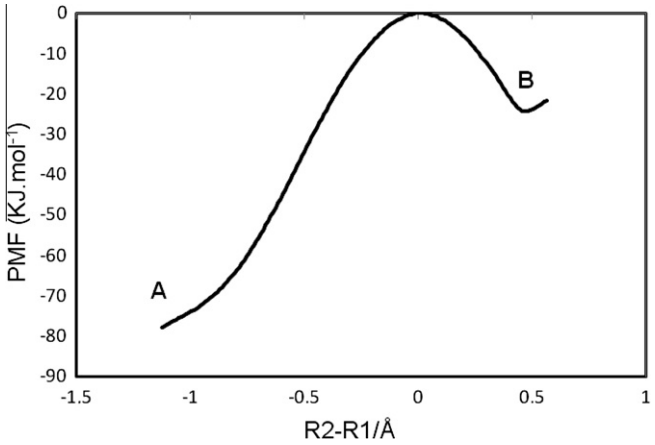

Figure 1. Potential of mean force profile for proton transference from Asp214 to Asp34 (transformation between **A** and **B** forms). Relative energies in kJ mol^{-1} and reaction coordinate (R1–R2) in Å.

3. Results and discussion

3.1. pK_a calculations

As mentioned in the previous section, we performed pK_a calculations for PM IV complexed with the KNI-764 inhibitor using 'cluster methods' and *propKa,* once standard pK_a values of ionisable groups can be shifted by the local protein environment. According to these methods, the Asp214 residue was found to be protonated, while Asp34 residue was found be deprotonated (Supporting information). Interestingly, Asp214 and Asp34 have been proposed as

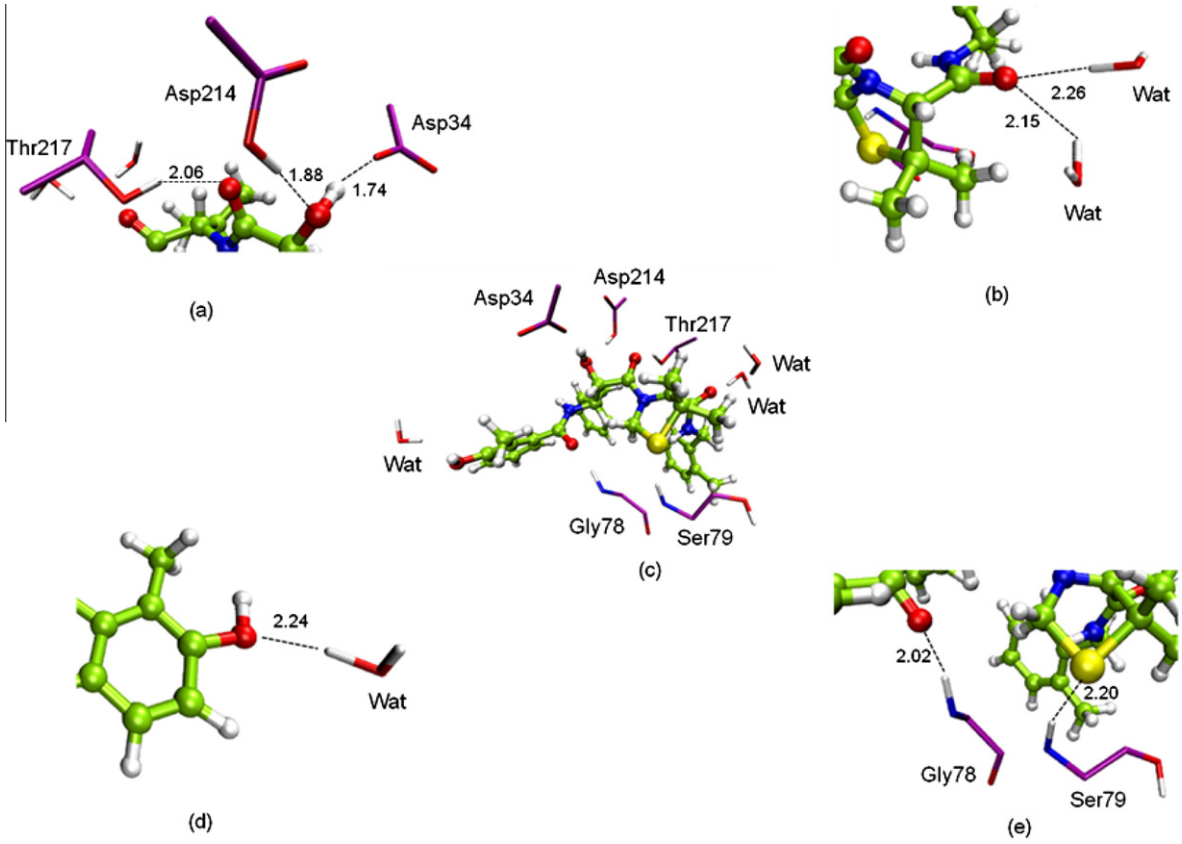

Figure 2. Details of interaction between KNI-764 and key residues obtained after 1.6 ns of AM1/MM MD simulations and representation of the most important interactions (key interatomic distances, in Å) for **A** form: (a) KNI-764 and Asp34, Asp214 and Thr217; (b) KNI-764 and two waters; (c) structure of PM IV–KNI-764 complex showing all key residues; (d) KNI-764 and one water and (e) KNI-764 and Gly78 and Ser79.

the catalytic residues, one of which is protonated while the other is negatively charged. Thus the correct protonation state for both of these residues is essential for a realistic modeling of the binding site [11]. Consequently, we have considered the PM IV–KNI-764 complex using two states of protonation, Asp214 (model **A**) and Asp34 (model **B**) protonated (see Scheme 1). These results are qualitatively in agreement, predicting the same protonation state for a number of residues at the selected pH of the simulations. Thus, according to these results, most residues were found in their standard protonation state.

3.2. Protonation state of PM IV

Protonation of the catalytic residues in PMs enzymes is directly associated with the presence and type of inhibitor bound; thus it can be concluded that there is a unique model capable of satisfactorily describing the protonation state of key aspartates such as Asp214 and Asp34 [14,18]. In the present study, electrostatic contribution to the free energy in the protein–substrate interaction, obtained from the free energy perturbation (FEP) calculations at AM1/MM level for **A** and **B** models reveals that a more stable form of PM IV–KNI-764 is obtained from protonation of Asp214 residue, which is consistent with the literature [14,18]. The difference observed between these models is 11.12 kJ mol^{-1} (Table 1). Obviously, the FEP calculation is only one of the electrostatic contributions to the total binding free energy. We also calculated protein interaction energies Elect-AM1/MM computed during the last 100 ps of AM1/MM MD simulations (Table 1). The result reveals that a more stable form of PM IV–KNI-764 was obtained when Asp214 was considered protonated. Thus, we can conclude that different methodologies presented the same tendencies, in accordance with the literature [14].

Based on the results and observations described above, we decided to trace the potential of mean force (PMF) corresponding to the proton transfer from the carboxylate oxygen atom OD1 of Asp214 to carboxylate oxygen atom OD2 of Asp34 (transformation from **A** to **B** form). As shown in the PMF profile (Figure 1), inhibitor–protein complex is more stable in the **A** form than in the **B** form by about 55 kJ mol^{-1}, in accordance with the results of binding free energies. The free energy barrier for the **A** to **B** conversion is 80 kJ mol^{-1}. Thus, this result indicates that the protonation of Asp214 favors a stable active site structure. This result is in agreement with previous HB analysis, which showed that the protonation of Asp214 is more consistent with the crystallographic data, which report the catalytic mechanism [14]. These findings are also in agreement with our previous QM/MM MD studies of interactions of EH58 inhibitor with PM II protein [34].

3.3. PM IV–KNI-764 complex

The contributions of individual results for more stable PM IV–KNI-764 complex (**A** form, obtained from protonation of Asp214 residue) are discussed below and the results for **B** form are discussed in Supporting Information.

In accordance with the results of the MD simulations of QM/MM, diverse interaction keys have been found between PM IV and KNI-764 inhibitor. As can be seen from **A** model (Figure 2a), the hydroxyl group interacts with the OD2 oxygen atom of Asp34 (1.74 Å) through a hydrogen bond. Moreover, the hydroxyl group also presents a hydrogen bond interaction with acid aspartic protonated Asp214 (1.88 Å).

As observed in Figure 2c, other important residues present a favorable interaction with the ligand, such as Gly78, Ser79 and Thr217. The amino group of Gly78 and Ser79 residues interacts with KNI-764 forming hydrogen bond at 2.02 and 2.20 Å in **A** model (Figure 2e). The hydroxyl group of Thr217 form hydrogen bonds with inhibitor at 2.06 Å in **A** model (Figure 2a).

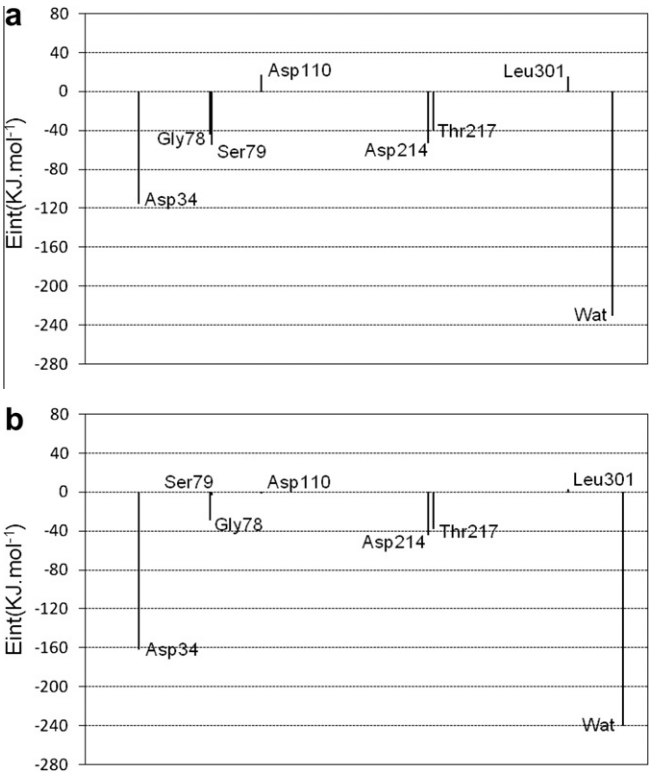

Figure 3. (a) Contributions of individual amino acid residues to inhibitor interaction energy (in kJ mol^{-1}) computed during the last 100 ps of AM1/MM MD simulations for **A** form (a) and (b) computed using DFT/MM from structures optimized after 1.6 ns B3LYP/MM MD simulations for **A** form (in kJ mol^{-1}).

Contributions of individual amino acid residues to inhibitor interaction energy obtained with AM1/MM for model **A** are shown in Figure 3a, where negative values correspond to stabilization and positive values correspond to destabilization of the protein–inhibitor complex. In this study, we also performed calculations with B3LYP/MM in order to evaluate the appropriateness of the AM1/MM potentials for describing the contributions of individual residues between the inhibitor and the protein (Figure 3b). The results show that both AM1/MM and B3LYP/MM calculations produce similar results. Analyzing the Figure 3, one may again clearly observe the presence of all amino acids cited above, showing how the interactions between the residues are consistent with those found in the literature [14].

In addition, we observe in Figure 2 that there are additional water molecules that interact with the inhibitor stabilizing the complex enzyme–inhibitor for **A** model (Figure 3). Three water molecules are involved in hydrogen bonds with KNI-764 in the **A** model (Figure 2b and d). Recent reports have proposed that water molecules are important for stabilizing the interaction between the ligand and the PMs enzymes class [18], in accordance with our theoretical simulations.

Finally, The catalytic aspartate protonation state has a strong influence on the presence or absence of the hydrogen bonds between some residues [14,18]. As can be observed in Figures 2 and 3 and Supporting Information (Figures S3 and S4), the hydrogen bond in **A** and **B** models and inhibitors are practically equal. Nevertheless, comparison between both models would require simulation of the proton-transfer step from Asp214 to Asp34 or vice versa, as discussed above.

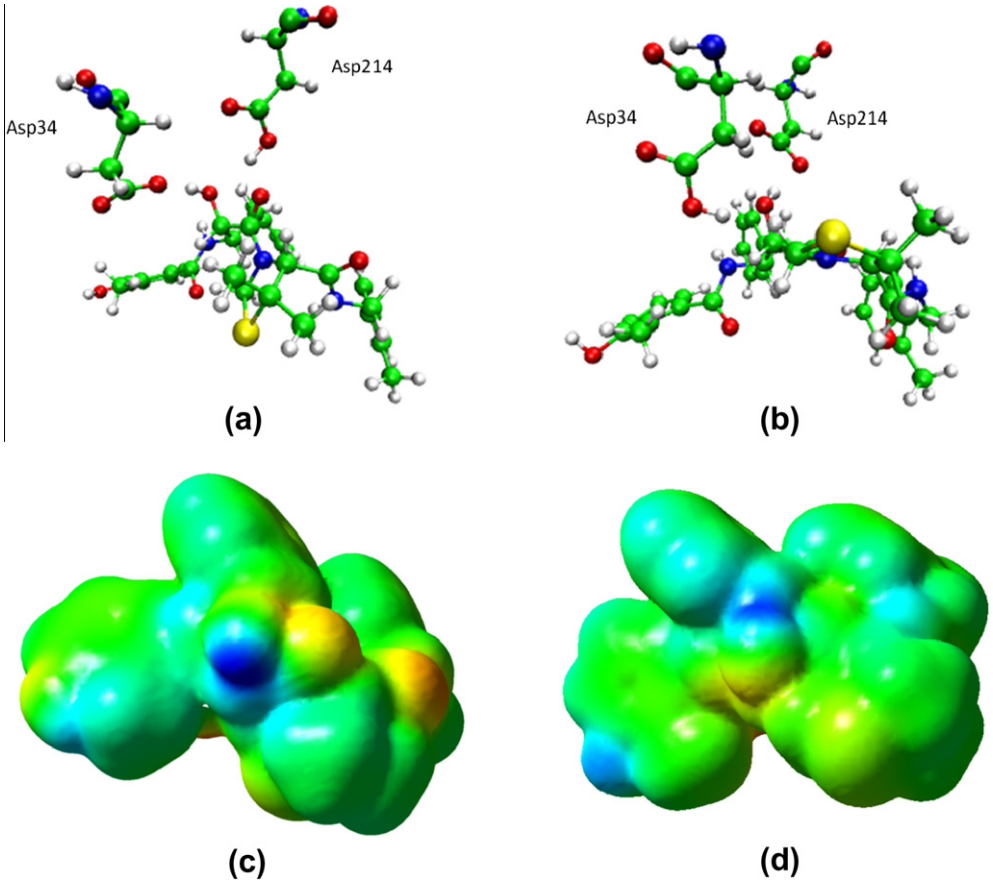

Figure 4. MEP surfaces of (a) **A** form and (b) **B** form. The increase of negative charges goes from blue (positive) to red (negative). (For interpretation of references to color in this figure legend, the reader is referred to the web version of this article.)

3.4. Mep

The Molecular Electrostatic Potential (MEP) is highly informative of the nuclear and electronic charge distribution of a given molecule. MEP has been applied in studying biological interactions and definition of molecular reactivity patterns [35,36]. In this study, the MEP surfaces were computed under the effect of the protein environment and were derived from B3LYP/6-31G (d) calculations using Gaussian 03 [37] and visualized in Gaussview 3.07 [38]. These surfaces correspond to an isodensity value of 0.002 a.u. It is interesting to highlight the noncovalent interactions occurring at the molecular surface. In Figure 4, the most nucleophilic regions (negative electronic potential) are in red, while the most electrophilic regions (positive electrostatic potential) appear in blue. In the **A** model, the nucleophilic region, can be found around the cetone group of the inhibitor (Figure 4a). The electrophilic regions for the **A** model can be found around the hydrogen atoms, mainly on atom H linked to the oxygen atom (hydroxyl group) matching the positions of Asp214 and Asp34, respectively. The positive region around the H atom (hydroxyl group) is more positive in the **A** model, because the hydroxyl group interacts with the OD2 oxygen atom of Asp34 (1.74 Å) through a hydrogen bond. The nucleophilic region can be found around the carbonyl groups of the inhibitor, matching the positions of Gly78 and Ser79. These residues interact with the inhibitor, forming a hydrogen bond as seen in previous section. These MEPs are in accordance with our results regarding contributions of individual amino acid residues to inhibitor interaction and may be used as templates for design of new inhibitors against malaria.

4. Conclusions

In the research reported here, hybrid QM/MM MD simulations have been carried out for PM IV complexed with KNI-764 using two different forms for catalytic residues in the complex formed; Asp214 protonated or Asp34 protonated (**A** and **B** models). The analysis of individual interactions between the inhibitor and the amino acids of the enzyme active site reveals how the influence of Asp34, Gly78, Ser79, Asp214 and Thr217 appears to be crucial, with the interactions established between the inhibitor and theses residues being especially important. Moreover, the calculations that determined the electrostatic contribution to the protein–ligand interaction free energies show that prevalence of the **A** form is a better model for this inhibitor in the active site of PM IV. The PMF profile of the proton transfer between the carboxylate oxygen atom of Asp214 to the carboxylate oxygen atom of Asp34 for inhibitor–protein complex shows that the **A** form is more stable than the **B** form in accordance with the binding free energy results. The results reported here are in agreement with the literature, which demonstrates the efficiency of applying in this methodology. Finally, the results are expected to provide useful information for the rational design of new PM IV inhibitors.

Acknowledgements

We would like to thank the *Coordenação de Aperfeiçoamento de Pessoal de Nível Superior* (CAPES), *Conselho Nacional de Desenvolvimento Científico e Tecnológico* (CNPq), *Fundação de Amparo e Desenvolvimento da Pesquisa* (FADESP) and *Pró-Reitoria de Pesquisa*

e Pós-Graduação of Universidade Federal do Pará (PROPESP-UFPA) for financial support.

Appendix A. Supplementary data

Supplementary data associated with this article can be found, in the online version, at doi:10.1016/j.cplett.2011.04.085.

References

[1] M. Schlitzer, Chem. Med. Chem. 2 (2007) 944.
[2] WHO: fact sheet N8 94 (2007) available online: <http://www.rollbackmalaria.org>.
[3] S.E. Francis, D.J. Sullivan, D.E. Goldberg, Annu. Rev. Microbiol. 51 (1997) 97.
[4] S. Bjelic, M. Nervall, H. Gutierrez-de-Teran, K. Ersmark, A. Hallberg, J. Aqvist, Cell. Mol. Life Sci. 64 (2007) 2285.
[5] D.E. Goldberg, A.F.G. Slater, R. Beavis, B. Chait, A. Cerami, G.B. Henderson, J. Exp. Med. 173 (1991) 961.
[6] R. Banerjee, J. Liu, W. Beatty, L. Pelosof, M. Klemba, D.E. Goldberg, Natl. Acad. Sci. USA 99 (2002) 990.
[7] N.K. Bernstein, M.M. Cherney, C.A. Yowell, J.B. Dame, M.N.G. James, J. Mol. Biol. 329 (2003) 505.
[8] S.E. Francis et al., Embo J. 13 (1994) 306.
[9] J.C. Clemente et al., Acta Crystal. Sec. D Biol. Crystal. 62 (2006) 246.
[10] A. Nezami et al., Biochemistry 42 (2003) 8459.
[11] Y. Kiso, H. Matsumoto, S. Mizumoto, T. Kimura, Y. Fujiwara, K. Akaji, Biopolymers 51 (1999) 59.
[12] T. Mimoto, J. Imai, S. Kisanuki, H. Enomoto, N. Hattori, K. Akaji, Y. Kiso, Chem. Pharm. Bull. 40 (1992) 2251.
[13] H.M. Abdel-Rahman et al., Biol. Chem. 385 (2004) 1035.
[14] H. Gutierrez-de-Teran, M. Nervall, B.M. Dunn, J.C. Clemente, J. Aqvist, Febs Lett. 580 (2006) 5910.
[15] S. Bjelic, J. Aqvist, Biochemistry 45 (2006) 7709.
[16] H. Gutierrez-de-Teran et al., Biochemistry 45 (2006) 10529.
[17] A. Kiriyama, T. Mimoto, Y. Kiso, K. Takada, Biopharm. Drug Disp. 14 (1993) 199.
[18] R. Friedman, A. Caflisch, Febs Lett. 581 (2007) 4120.
[19] C.N. Alves, S. Marti, R. Castillo, J. Andres, V. Moliner, I. Tunon, E. Silla, Chem. A Eur. J. 13 (2007) 7715.
[20] H.M. Senn, W. Thiel, Ang. Chem. Int. Ed. 48 (2009) 1198.
[21] J.L. Gao, X.F. Xia, Science 258 (1992) 631.
[22] J. Antosiewicz, J.A. McCammon, M.K. Gilson, J. Mol. Biol. 238 (1994) 415.
[23] M.K. Gilson, Proteins 15 (1993) 266.
[24] H. Li, A.D. Robertson, J.H. Jensen, Protein Struct. Funct. Bioinf. 61 (2005) 704.
[25] M.J. Field, P.A. Bash, M. Karplus, J. Comput. Chem. 11 (1990) 700.
[26] M.J.S. Dewar, E.G. Zoebisch, E.F. Healy, J.J.P. Stewart, J. Am. Chem. Soc. 107 (1985) 3902.
[27] W.L. Jorgensen, D.S. Maxwell, J. TiradoRives, J. Am. Chem. Soc. 118 (1996) 11225.
[28] W.L. Jorgensen, J. Chandrasekhar, J.D. Madura, R.W. Impey, M.L. Klein, J. Chem. Phys. 79 (1983) 926.
[29] M.J. Field, M. Albe, C. Bret, F. Proust-De Martin, A. Thomas, J. Comput. Chem. 21 (2000) 1088.
[30] J. Lameira, C.N. Alves, V. Moliner, S. Marti, N. Kanaan, I. Tunon, J. Phys. Chem. B 112 (2008) 14260.
[31] C.T. Lee, W.T. Yang, R.G. Parr, Phys. Rev. B 37 (1988) 785.
[32] D.A. McQuarrie, Statistical Mechanics, Haper & Row, New York, 1976. p. 266.
[33] B. Roux, Comput. Phys. Commun. 91 (1995) 275.
[34] N.F. Silva, J. Lameira, C.N. Alves, J. Mol. Mod. doi:10.1007/s00984-011-0963-1.
[35] A. Gavezotti, J. Am. Chem. Soc. 105 (1983) 5220.
[36] E. Cubero, F.J. Luque, M. Orozco, Proc. Natl. Acad. Sci. 95 (1998) 5976.
[37] M.J. Frisch et al., Gaussian 03 Revision C.02, Gaussian Inc., Wallingford CT, 2004.
[38] R. Dennington, T. Keith, J. Millam, K. Eppinnett, W.L. Hovell, R. Gilliland, GaussView V3.0, Semichem Inc.: Shawnee Mission, KS, 2003.